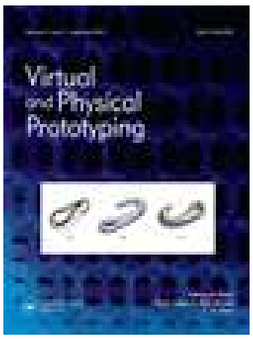

Virtual and Physical Prototyping

ISSN: 1745-2759 (Print) 1745-2767 (Online) Journal homepage: www.tandfonline.com/journals/nvpp20

Evaluation of *in vitro* degradation of PCL scaffolds fabricated via BioExtrusion – Part 2: Influence of pore size and geometry

The present study is to accurately investigate the influence of design parameters, such as filament distance (FD) and lay-down pattern, on the degradation behaviour and kinetics of PCL scaffolds, obtained via BioExtrusion

M. Domingos, F. Chiellini, S. Cometa, E. De Giglio, E. Grillo-Fernandes, P. Bartolo & E. Chiellini

To cite this article: M. Domingos, F. Chiellini, S. Cometa, E. De Giglio, E. Grillo-Fernandes, P. Bartolo & E. Chiellini (2011) Evaluation of *in vitro* degradation of PCL scaffolds fabricated via BioExtrusion – Part 2: Influence of pore size and geometry, Virtual and Physical Prototyping, 6:3, 157-165, DOI: 10.1080/17452759.2011.605839

To link to this article: https://doi.org/10.1080/17452759.2011.605839

Published online: 10 Oct 2011.

Virtual and Physical Prototyping, Vol. 6, No. 3, September 2011, 157–165

Taylor & Francis
Taylor & Francis Group

Evaluation of *in vitro* degradation of PCL scaffolds fabricated via BioExtrusion – Part 2: Influence of pore size and geometry

The present study is to accurately investigate the influence of design parameters, such as filament distance (FD) and lay-down pattern, on the degradation behaviour and kinetics of PCL scaffolds, obtained via BioExtrusion

M. Domingos[a]*, F. Chiellini[b], S. Cometa[b], E. De Giglio[c], E. Grillo-Fernandes[b], P. Bartolo[a] and E. Chiellini[b]

[a]Centre for Rapid and Sustainable Product Development, Polytechnic Institute of Leiria (IPL) Leiria, Portugal
[b]Laboratory of Bioactive Polymeric Materials for Biomedical & Environmental Applications (BIOlab), Department of Chemistry & Ind. Chemistry, University of Pisa, Pisa, Italy
[c]Department of Chemistry, University of Bari, Bari, Italy

(*Received 13 July 2011; final version received 14 July 2011*)

The *in vivo* degradation processes by which scaffolds degrade and are replaced by neo-tissue are complex and may be influenced by many factors, including environmental conditions, material properties, porosity and 3D architecture. The present study is focused on the influence of design parameters, filament distance (FD) and lay-down pattern, on the degradation kinetics of Polycaprolactone (PCL) scaffolds obtained via BioExtrusion. Through the variation of design parameters it was possible to obtain two groups of scaffolds with distinct pore geometry and size. The *in vitro* degradation was performed in simulated body fluid (SBF) and in phosphate buffer solution (PBS) for six months. Our results highlight a more complex degradation pattern of the scaffolds in SBF than in PBS, probably related to a mineral deposition. Significant statistical differences in weight loss values at month 6, allowed us to conclude that degradation kinetics of PCL scaffolds is strongly influenced by the pore size.

Keywords: biomanufacturing; biomaterials; scaffolds; tissue engineering; extrusion

1. Introduction

Solid freeform (SFF) techniques are increasingly being recognised as ideal techniques to produce complex three-dimensional (3D) structures with optimal pore size and spatial distribution, using a wide range of materials, such as natural/synthetic polymers, ceramics, and composites.

Different techniques have been developed and employed with success to manufacture scaffolds for tissue engineering (TE) applications, including 3D printing, fused deposition modelling, stereolithography, selective laser sintering and a few other extrusion-based technologies, such as 3D plotting and 3D fibre-deposition (Hull 1990, Scott 1991, Bredt *et al.* 1998, Landers and Mulhaupt 2000, Landers *et al.* 2002a, 2002b, Malda *et al.* 2004, Woodfield *et al.* 2004, Moroni *et al.* 2005, Chu 2006, Moroni *et al.* 2006a, b, Gloria *et al.* 2009). The structures are built in a layer by layer manner starting from a 3D model of a specific object and controlled by a computer. This approach enables the production of customised scaffolds with very complex 3D shapes, reproducible internal/external architecture and interconnectivity, increasing mass transport of oxygen and nutrients

*Corresponding author. Email: marco.domingos@ipleiria.pt

Virtual and Physical Prototyping
ISSN 1745-2759 print/ISSN 1745-2767 online
http://www.tandfonline.com
http://dx.doi.org/10.1080/17452759.2011.605839

throughout the entire scaffold and providing an adequate biomechanical environment for tissue regeneration while shaping the defect or injury. In order to successfully design and produce scaffolds, especially when using bioresorbable polymers, one should always ensure that the degradation rate of the structure matches the rate of tissue growth. Despite all variables possible of being manipulated to fulfil this requirement, it is widely accepted that the porous architecture of a scaffold is a critical parameter, since the degree of vascular ingrowth that occurs *in vivo* is closely related to this feature (Kim *et al.* 2000). However, to date, no consensus has been found regarding the mechanism and to which extent, pore size and geometry actually influence the degradation behaviour of a scaffold designed to regenerate a specific tissue. Therefore, more accurate and systematic studies must be conducted by considering a series of complex phenomena that occur in the native environment.

In this respect, a novel extrusion-based system that is known as BioExtruder was employed to fabricate Polycaprolactone (PCL) scaffolds characterised by a homogeneous spatial distribution of pores and fully interconnected internal channels. The potential and feasibility of the instrument in developing scaffolds for TE has already been demonstrated by the authors in previous works (Domingos *et al.* 2009a, 2009b).

The flexibility and versatility of this extrusion-based technology, opened the opportunity to study with a high level of accuracy how structural features (lay-down pattern and filament distance [FD]), influenced the degradation kinetics of the fabricated devices.

Figure 1. BioExtruder Device.

As demonstrated by the authors in the previous article, a more complex degradation pattern was observed when simulated body fluid (SBF) medium was employed (Domingos *et al.* 2010). The wettability measurements performed on PCL

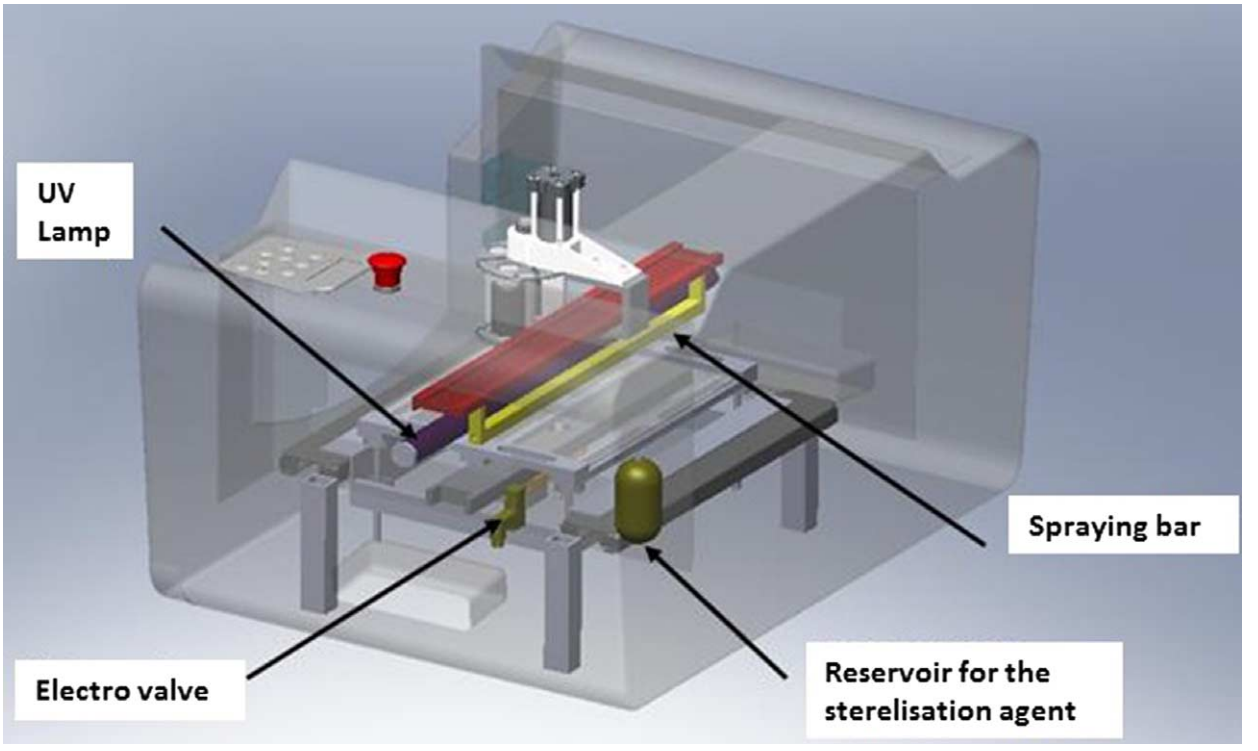

Figure 2. Representation of the sterilisation system.

Table 1. Processing conditions.

Processing conditions	
Reservoir temperature (°C)	80
Extrusion chamber temperature (°C)	80
Screw rotation velocity (rpm)	30
Deposition velocity (mm/s)	10
Extrusion pressure (bar)	4
Nozzle diameter (μm)	300
Slice thickness (ZZ increment) (μm)	300

scaffolds revealed that the degradation process was still in an early stage. These results confirm that the degradation kinetics of PCL (both in PBS and SBF) is strongly influenced by its crystallinity and hydrophobicity. Despite that, some preliminary conclusions regarding the influence of pore size and shape on the degradation kinetics of structures can be drawn. It was found that, after degradation in both the media, PCL wettability increased, probably due to the formation of surface free carboxylic groups as a result of the ester linkages scission.

Experimental work is in progress in order to provide a better insight into the effect of the design parameters on the degradation kinetics of 3D PCL scaffolds under accelerated conditions (NaOH).

2. Materials and methods

2.1 *Materials*

CAPA® 6500 poly(ε -caprolactone) in the form of pellets with molecular weight around 50.000 was supplied by Perstorp UK Ltd (Cheshire, United Kingdom). SBF and PBS were prepared as previously reported (Domingos *et al.* 2010).

2.2 *Scaffolds design and fabrication*

Three-dimensional (3D) PCL scaffolds were produced employing the BioExtruder, a novel biomanufacturing system under development at the Polytechnic Institute of Leiria (IPL, PT) for tissue engineering applications (Figure 1).

A detailed description of the instrument along with the flowchart information required for the fabrication of 3D scaffolds for TE can be found elsewhere (Domingos *et al.* 2009a, 2009b, Almeida *et al.* 2010).

Some improvements have been made with regard to the previous version, namely the introduction of a direct sterilisation system comprised of a UV lamp and a spraying system that enables the sterilisation of the produced structures (Figure 2). A new extrusion head has also been developed, with a shorter screw, in order to ease the extrusion of materials with higher density.

Briefly, rectangular prisms measuring 30 (length) x 30 (width) $\times$ 8 mm (height) were initially designed using a computer-aided design (CAD) software (SolidWorks, Dassault Systèmes S.A.). Afterwards, imposing a single lay-down pattern of 0/90° and varying FD values from 450 to 650 μm, it was possible to produce scaffolds with square interconnected pores of different dimensions and porosity levels.

Regarding pore shape, three lay-down-patterns were adopted (0/90°, 0/60/120° and 0/45/90/135°) maintaining a regular FD of 650 μm, resulting in scaffolds with quadrangular, triangular and complex polygonal internal pore geometries, respectively.

Processing conditions were defined based on previous experiments and maintained constant during the fabrication process (Table 1).

All of the specimens were then cut into smaller blocks of the required dimensions for further analyses.

2.3 *Scaffolds characterisation*

2.3.1. Fourier-transform infrared spectroscopy (FT-IR)

All of the six typologies of scaffolds, as well as the pristine PCL sample, were dissolved in chloroform and cast on KBr plates, in order to ascertain that the new conditions of extrusion and especially of sterilisation did not alter the chemical nature of the polymer. FT-IR spectra were acquired on a Perkin-Elmer 1600 x FTIR spectrometer.

2.3.2. Scanning electron microscopy (SEM)

The morphology of the scaffolds, namely the pore size and surface topography of the filaments, were assessed by means of SEM, using a JEOL (JSM5600LV, Tokyo, Japan) scanning electron microscope. Samples were air dried and gold sputtered under high vacuum.

2.4 *Degradation assay*

The methodology adopted for the degradation tests has already been described in detail elsewhere (Domingos *et al.* 2010). Briefly, three specimens of each scaffold topology, after being sterilised with UV radiation for 30 min (BioExtruder sterilisation system), were cut into smaller samples, measuring 4 x 4 x 3 mm, and immersed in PBS or SBF solutions (37°C, pH 7.4) for a period of six months.

At intervals of one month, scaffolds were withdrawn from the degradation media and immersed for some days in Millipore water in order to remove excess of salts, carefully wiped, dried under vacuum for 12 h at room temperature and weighed (W_t). The weight loss percentage ($WL\%$) was determined by the following equation:

$$WL\% = \frac{(W_0 - W_t)}{W_0} \times 100 \qquad \text{Equation (1)}$$

Table 2. Porosity of the scaffolds produced with different lay-down patterns.

Lay-down pattern (°)	FD (μm)	Porosity (%)
0/90	650	51
0/60/120	650	48
0/45/90/135	650	45

2.5 *Characterisation of the degraded scaffolds*

2.5.1. Size exclusion chromatography (SEC)

The weight and number average molecular weights (M_w and M_n, respectively) and polydispersity index (PDI) of the scaffolds having different pore geometries and sizes, before (time = T0 months) and after degradation (time = T6 months), both in SBF and PBS, were obtained using SEC, using a Jasco PU-1580 High-performance liquid chromatography (HPLC) liquid chromatograph pump connected to Jasco 830-RI detector, and equipped with two Mixed-D PLgel columns (300 x 7.5 mm). Chloroform was used as the eluent and the calibration curve was established by using mono-dispersed polystyrene (PS) standards (Perkin-Elmer). The PS calibration was converted into one for PCL using universal calibration, as already specified by the authors (Domingos *et al.* 2010).

2.5.2. Differential scanning calorimetry (DSC)

Changes in thermal properties of the scaffolds as a function of the degradation medium and topology were evaluated by DSC. Measurements were performed using a Mettler DSC 822^C module with FRS5 sensor and operated by means of STAR software. Samples of 10–15 mg were scanned from -100°C to 100°C comprising first and second heating and first cooling under nitrogen atmosphere, at a rate of 10 °C/min.

2.5.3. Static Contact Angle (SCA) measurements

Static contact angle (SCA) measurements were performed on PCL films, before and after degradation, obtained by spin coating of PCL scaffolds in solution with chloroform. An HPLC grade water sessile drop method at 25 ± 0.1 °C with a Drop Shape Analysis System (DSA) 10 drop shape analysis system (Kruss, Hamburg, Germany) was employed. The polymer solution 0.1% wt was initially filtered using a 0.45 μm nylon filter, dropped on the surface of a microscope glass plate and spin coated at 6200 rpm for 60 s. The films were kept in a dry atmosphere for further analysis. Average data was obtained with nine measurements.

Table 3. Porosity of the scaffolds produced with different filament distances.

FD (μm)	Lay-down pattern (°)	Porosity (%)
650	0/90	51
550	0/90	34
450	0/90	23

2.6 *Statistical data treatment*

Degradation experiments were carried out with at least three replicates, which were identically treated and processed. Contact angle measurements were performed over nine replicates. Relative changes of the assessed properties were statistically analysed with a $P < 0.05$ significance level using a one-way analysis of variance (ANOVA), using Tukey's test and the error of mean was calculated as standard deviation.

3. Results and discussion

The *in vitro* degradation assay was performed on PCL scaffolds fabricated with three lay-down patterns and three different pore sizes. The aim of this study was to investigate the variation of degradation kinetics associated with the variation of scaffold architecture and porosity, and ultimately to determine the suitability of the structures for specific tissue engineering applications. The degradation phenomenon was evaluated through the change in physical (mass), thermal (crystallinity) and chemical (molecular weight) properties of the scaffolds.

3.1 *Scaffold design and fabrication*

PCL scaffolds were produced via BioExtrusion applying different lay-down patterns and filament distances resulting in structures with different geometries and pore sizes, respectively.

The porosity of the structures was evaluated using the following methodology: (1) measuring the weight and volume of each sample, (2) calculating the apparent density of the PCL scaffolds, (3) applying the following equation:

$$Porosity = \left(1 - \frac{\rho*}{\rho_{Sub}}\right) \times 100 \qquad \text{Equation (2)}$$

where ρ* is the apparent density of the cellular structure (scaffold) and ρ_{sub} is the density of the original substance ($\rho_{sub} = 1145 g/cm^3$).

The porosities of the produced scaffolds are listed in Table 2 and Table 3.

3.2 *Morphological characterisation*

Morphological evaluation of the structures was carried out under scanning electron microscopy (SEM). As confirmed by Figure 3, PCL scaffolds produced by applying a constant FD of 650 μm and three different lay-down patterns of 0/90°, 0/60/120° and 0/45/90/135°, resulted in structures

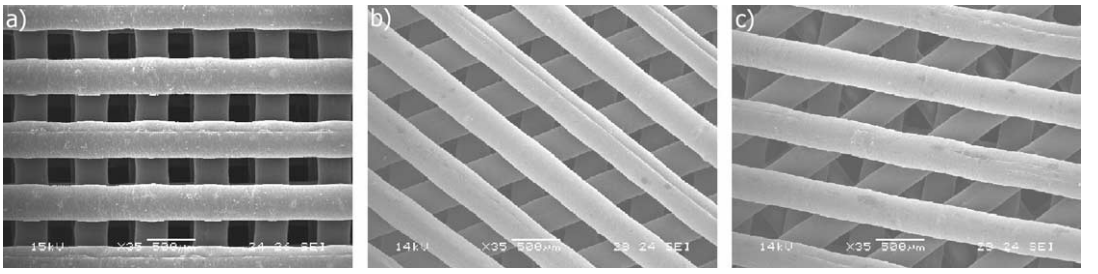

Figure 3. Scaffolds produced varying the lay-down pattern. a) 0/90. b) 0/60/120°. c) 0/45/90/135°.

with quadrangular, triangular and complex polygonal pores, respectively.

The influence of user-defined design parameter, FD was also studied. The scaffolds were developed with a single lay-down pattern of 0/90° and a series of FD's, namely 650, 550 and 450 μm. SEM observations revealed that the variation of FD strongly influences the pore size and porosity of the 3D structures. In other words, by increasing the FD it was possible to observe an increment of pore size and consequently the porosity (Figure 4).

The cross-sectional views of the SEM images revealed the complete interconnectivity and structural integrity of the internal channel networks (data not shown).

3.3 *FT-IR analysis*

Potential chemical/physical modifications of PCL, caused by the extrusion process were previously excluded by Gel Permeation Chromatography (GPC), Differential Scanning Calorimetry (DSC) (Domingos *et al.* 2009a) and X-ray photoelectron spectroscopy (XPS) (Domingos *et al.* 2010) investigations. In order to confirm that the improvements made in the BioExtruder, namely the introduction of a new extrusion head and sterilisation system, as well the employment of a wide variety of processing conditions, did not cause any degradation/modification of the polymer, FT-IR analysis was carried out both on the pristine PCL material and all of the six scaffold's typologies.

In all cases, an almost similar FT-IR spectrum for the scaffold and the pristine material was recorded, displaying typical adsorption bands of PCL (*i.e.* the –C(=O)O– stretching vibrations at 1243 cm^{-1} and the strong C=O stretching band at 1725 cm^{-1}).

For clarity, the FT-IR spectrum of only one typology of scaffold is reported in Figure 5, in comparison with the spectrum of the pristine material employed for extrusion process.

3.4 *In vitro degradation*

As previously mentioned, degradation experiments were performed on PCL scaffolds having different pore sizes and shapes, using two different degradation media. As far as the PBS media is concerned, all investigated scaffolds, independently of pore size/shape, retained their framework and 3D morphology until the end of the experiment, which means that the degradation process was still in its early stage. Regarding weight loss percentage (%WL), no particular trend was deciphered hence suggesting an erosion degradation mechanism occurring on the surface of the scaffolds. Only negligible mass losses (< 0.5%) were observed during the whole degradation period of six months, regardless of the scaffold's 3D structure (Figure 6 and Figure 7).

Due to the high crystallinity and hydrophobicity of the polymer, the degradation of PCL scaffolds in PBS remained very low, which did not enable an accurate comparison between the different topologies.

On the other hand, when the same scaffolds were immersed in SBF, it was possible to observe an initial

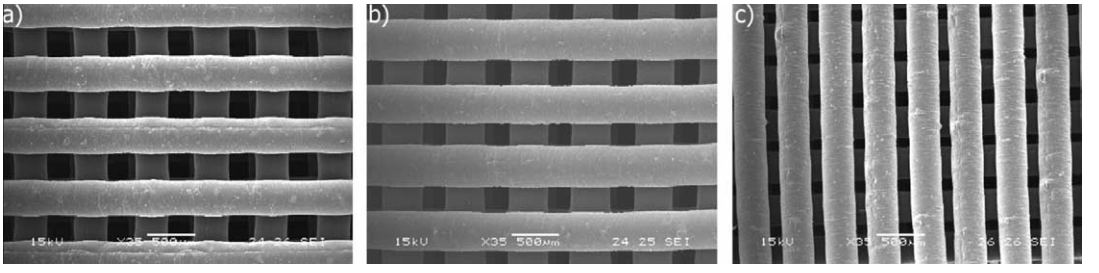

Figure 4. Scaffolds produced with different FDs. a) FD = 0.65 mm. b) FD = 0.55 mm. c) FD = 0.45 mm.

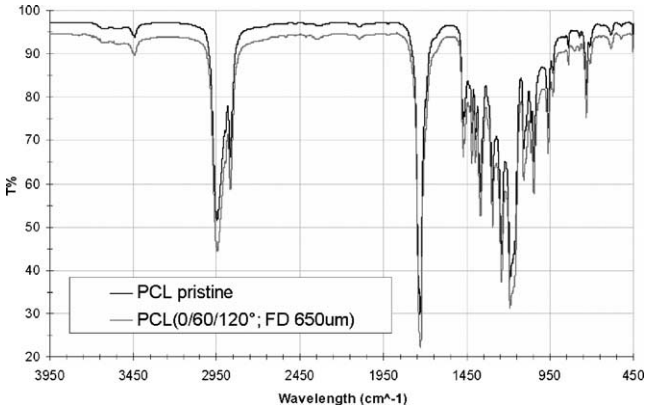

Figure 5. FT-IR spectra of PCL scaffold (0/60/120°, FD 650 μm) and of pristine PCL.

increase in the %WL, reaching a maximum value of 0.7% at month 2, followed by an apparent decrease in the following four months of degradation. It's important to underline that the concept of *apparent* WL% decrease herein described, is related to the mineral deposition that occurs on the surface of the scaffolds. This trend has already been observed in previous experiments performed by the authors and will be discussed in detail in the following sections (Domingos *et al.* 2010).

3.4.1. Statistical analysis

Statistical analysis was performed in order to verify the existence of significant differences in terms of %WL values at month 6 of degradation in SBF, between scaffolds produced with different lay-down patterns. The %WL values obtained did not present significant statistical differences ($P < 0.05$), indicating that, in the initial stages of degradation in SBF, the pore geometry does not have a strong influence on the degradation kinetics of the structures.

The same statistical test was carried out on scaffolds with different pore sizes and porosities. In this case, remarkable statistical differences ($P < 0.05$) were observed at month 6 of degradation. In particular, the lower the pore sizes, the higher the apparent %WL decrease. Interestingly, by this data, we can hypothesise that the reduction in pore size is responsible for at least one of these two processes: (1) an increase in mineral phase deposition and/or (2) a decrease in the degradation kinetics.

Therefore, general considerations can be drawn regarding the influence of pore size/shape, on the degradation kinetics of PCL scaffolds in SBF: (1) The mineral deposition process is strongly influenced by the pore size (smaller pores facilitate a higher mineral deposition). The contribution of the pore shape to this phenomenon appears to be negligible. (2) A highly porous scaffold (bigger pore size), presenting a higher

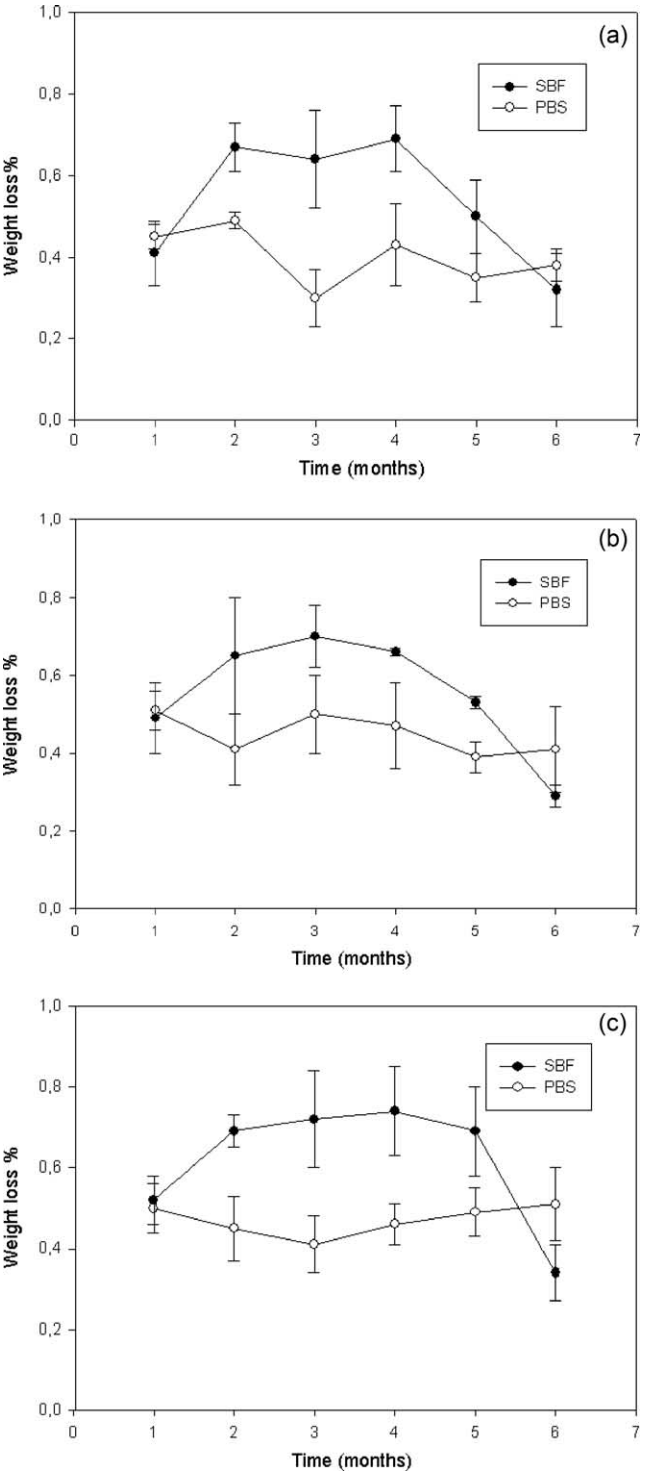

Figure 6. Percentage of weight loss variation, in SBF and PBS, of scaffolds produced with different lay-down patterns. a) 0/90. b) 0/60/120°. c) 0/45/90/135°.

surface area, can degrade more rapidly than a less porous one. Once again, no significant influence on degradation kinetics was observed by varying the geometry of the pores.

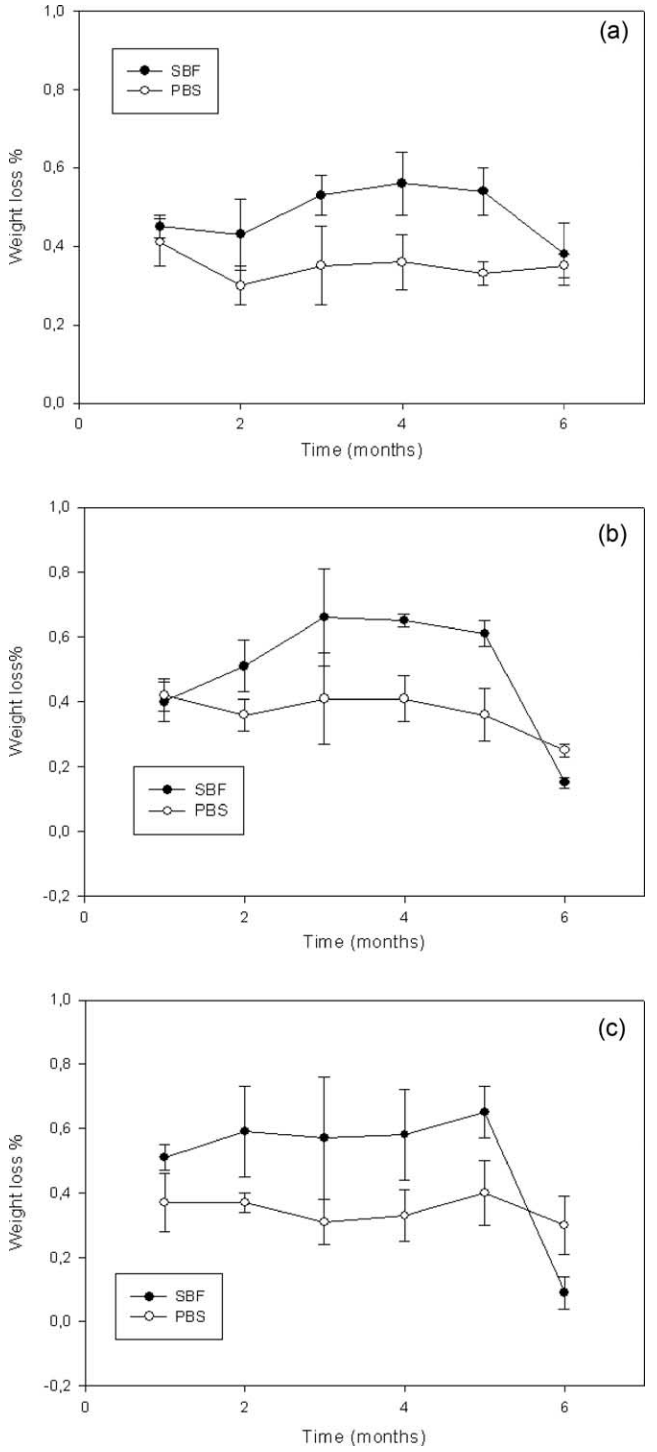

Figure 7. Percentage of weight loss variation, in SBF and PBS, of scaffolds produced with different FDs. a) FD = 650 μm. b) FD = 55 μm. c) FD = 450 μm.

3.4.2. Size exclusion chromatography (SEC)

The latter consideration was further supported by analysing the decrease in molecular weight of the degraded scaffolds.

Table 4. SEC data of PCL scaffolds as a function of the aqueous medium and lay-down pattern.

	PBS Media		SBF Media	
Lay-down pattern	M_n	PDI	M_n	PDI
0/90°	41400	1.33	40200	1.36
0/60/120°	42100	1.34	41500	1.34
0/45/90/135°	41900	1.35	42000	1.34

Tables 4 and 5 report the changes in the number average molecular weight (M_n) and polydispersity index (PDI) of PCL scaffolds, with different pore size/shape, degraded for six months in PBS and SBF.

Before degradation, all the scaffolds, independently of pore size/shape presented a M_n equal to (45600 ± 400) Da, with a PDI = 1.34.

By analysing the results reported in Table 4, it is possible to verify that PCL scaffolds produced with different lay-down patterns and comparable porosities, incubated in PBS and SBF media for six months, presented an almost similar degradation rate, resulting in a M_n decrease of $9.0 \pm 1.4\%$ and $10 \pm 2\%$ for PBS and SBF, respectively.

On the other hand, as illustrated in Table 5, a decrease in porosity (smaller pore size) led to a lower degradation rate, resulting in smaller percentages of M_n decrease at month six. For example, in the case of SBF, by reducing the FD from 550 μm to 450 μm it was possible to observe a M_n decrease of 6 and 2.4%, respectively. The same trend was found when the samples were incubated in PBS.

3.4.3. Differential scanning calorimetry (DSC)

Thermal properties of non-degraded and degraded PCL scaffolds (in PBS and SBF), with different pore topologies were investigated by means of DSC. All rapid prototyped scaffolds presented similar values of degree of crystallinity before degradation ($X_c = 57 \pm 2\%$). After six months of degradation, no significant differences in terms of X_c were found between the scaffolds with different pore sizes and geometries. Nevertheless, is worth highlighting that independently of pore configuration, a slight increment of X_c was observed in all samples after the degradation period, reaching $59 \pm 3\%$ and $62 \pm 2\%$ for PBS and SBF respectively.

3.4.4. Wettability measurements

Table 5. SEC data of PCL scaffolds as a function of the aqueous medium and filament distance.

	PBS Media		SBF Media	
Filament distance	M_n	PDI	M_n	PDI
650 μm	40700	1.36	39700	1.35
550 μm	43800	1.34	43000	1.34
450 μm	44900	1.34	44500	1.34

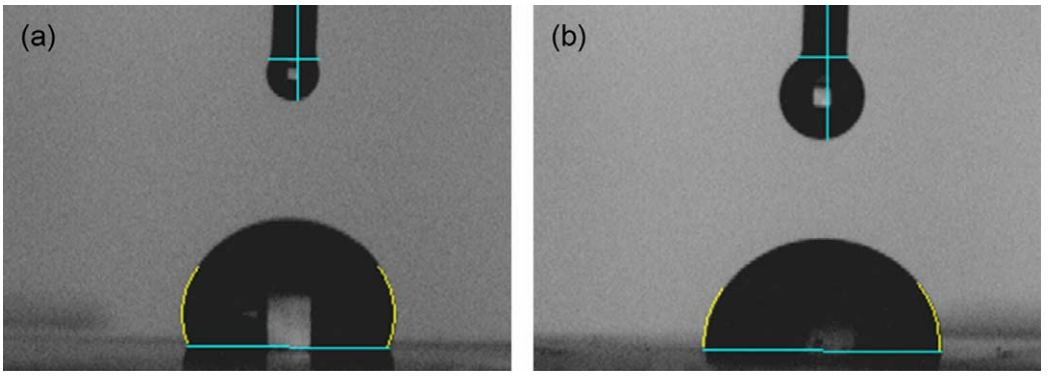

Figure 8. Contact angle photographs on undegraded (a) and PBS-degraded PCL cast films (b).

The static contact angles of PCL films were measured by dissolving in chloroform the undegraded and degraded PCL scaffolds with different geometries and pore sizes.

Spin coating onto glass coverslips can obviously introduce large differences between the molecular conformation, surface chemistry, surface energy, surface topology and porosity of the 3D scaffolds and the films. Moreover, the spin coating process can also be affected by the solvent employed in the film fabrication (Tang *et al.* 2004). Therefore, wettability results obtained for the films were not considered as reference values for the 3D scaffolds. Nevertheless, this analysis could supply information about the change in hydrophilicity which occurred as a consequence of the degradation. Water drops on both undegraded and six months PBS-degraded PCL surfaces are illustrated in Figure 8 (contact angles on SBF-degraded PCL did not differ from those on PBS and therefore the images are not presented).

The water contact angle for undegraded samples, regardless of the 3D architecture of the scaffolds, was equal to $106 \pm 5^{\circ}$. After degradation in PBS and SBF media for six months, the water contact angle decreased to $94 \pm 4^{\circ}$ and $93 \pm 3^{\circ}$ respectively. This confirmed that degradation of PCL involved a mechanism of surface erosion based on a random scission of polyester chains, in agreement with a previous work relevant to hydrolysis of PCL films in basic solution (Sun and Downes 2009). This scission seems to be consistent with an increase of free –COOH groups, which was in turn traduced in an increase of the material hydrophilicity and hence in a lower water contact angle.

4. Conclusions

In the present study the influence of design parameters, such as filament distance (FD) and lay-down pattern, on the degradation behaviour and kinetics of PCL scaffolds, obtained via BioExtrusion, was accurately investigated.

The *in vitro* degradation of the scaffolds was performed in SBF and in PBS solutions for six months. The degradation process increased the PCL wettability, as confirmed by contact angle measurements, performed both on undegraded and degraded samples. A more complex degradation pattern of the scaffolds was observed in SBF than in PBS, probably due to mineral deposition on the scaffold surface.

Finally, it is possible to conclude that pore size (porosity) has a stronger influence on the degradation kinetics of PCL scaffolds than pore geometry.

Acknowledgements

This work was performed within the framework of the European Network of Excellence "EXPERTISSUES" (Project NMP3-CT-2004-500283), with the partial financial support by Project PRIN – 2006 – prot. 2006038548. The authors wish to thank Mr. Piero Narducci in recording SEM images of scaffolds.

References

Almeida, H.A., *et al.*, 2010. *Processo e equipamento de fabrico rápido por bioextrusão*. Portuguese Patent Application 104247.

Bredt, J.F., *et al.*, 1998. *Three dimensional printing system*. United States Patent Application 5807437.

Chu, T.M.G., 2006. Solid freeform fabrication of tissue engineering scaffolds. *In*: P.X. Ma and J. Elisseeff, eds. *Scaffolding in tissue engineering*. Northwest Florida: Taylor and Francis, 139–153.

Domingos, M., *et al.*, 2010. Evaluation of in vitro degradation of PCL scaffolds fabricated via BioExtrusion-Part 1: influence of the degradation environment. *Virtual and Physical Prototyping*, **5** (2), 1–9.

Domingos, M., *et al.*, 2009b. BioExtruder: study of the influence of process parameters on PCL scaffolds properties. *In*: P.J. Bartolo, ed. *Innovative developments in design and manufacturing – advanced research in virtual and rapid prototyping*. London: Taylor & Francis, 67–73.

Domingos, M., *et al.*, 2009a. Polycaprolactone scaffolds fabricated via bioextrusion for tissue engineering applications. *International Journal of Biomaterials*, 2009, Article ID 239643.

Gloria, A., *et al.*, 2009. 3D fiber deposition technique to make multifunctional and tailor-made scaffolds for tissue engineering applications. *Journal of Applied Biomaterials & Biomechanics*, **7** (3), 141–152.

Hull, C., 1990. *Method for production of three–dimensional objects by Stereolithography*. United States Patent Application 4929402.

Kim, B-S., Baez, C.E., and Atala, A., 2000. Biomaterials for tissue engineering. *World Journal of Urology*, **18** (1), 2–9.

Landers, R., *et al.*, 2002b. Rapid prototyping of scaffold derived from thermoreversible hydrogels and tailored for application in tissue engineering. *Biomaterials*, **23** (23), 4437–4447.

Landers, R. and Mulhaupt, R., 2000. Desktop manufacturing of complex object, prototypes and biomedical scaffolds by means of computer-assisted design combined with computer-guided 3D plotting of polymers and reactive oligomers. *Macromolecular Materials and Engineering*, **282** (1), 17–21.

Landers, R., *et al.*, 2002a. Fabrication of soft tissue engineering scaffolds by means of rapid prototyping techniques. *Journal of Materials Science*, **37** (15), 3107–3116.

Malda, J., Woodfield, T.B. and van der Vloodt, F., 2004. The effect of PEGT/PBT scaffold architecture on the composition of tissue engineered cartilage. *Biomaterials*, **26** (1), 63–72.

Moroni, L., de Wijn, J.R. and Van Blitterswijk, C.A., 2005. Three-dimensional fiber-deposited PEOT/PBT copolymer scaffolds for tissue engineering: influence of porosity, molecular network mesh size and swelling in aqueous media on dynamic mechanical properties. *Journal of Biomedical Materials Research Part A*, **75** (4), 957–965.

Moroni, L., de Wijn, J.R. and Van Blitterswijk, C.A., 2006a. 3D fiber-deposited scaffolds for tissue engineering: influence of pores geometry and architecture on dynamic mechanical properties. *Biomaterials*, **27** (7), 974–985.

Moroni, L., *et al.*, 2006b. Dynamic mechanical properties of 3D fiber-deposited PEOT/PBT scaffolds: an experimental and numerical analysis. *Journal of Biomedical Materials Research Part A*, **78** (3), 605–614.

Scott, C.S., 1991. *Apparatus and method for creating three–dimensional objects*. United States Patent Application 5121329.

Sun, M. and Downes, S., 2009. Physicochemical characterisation of novel ultra-thin biodegradable scaffolds for peripheral nerve repair. *Journal of Materials Science: Materials in Medicine*, **20** (5), 1181–1192.

Tang, Z.G., *et al.*, 2004. Surface properties and biocompatibility of solvent-cast poly[(-caprolactone] films. *Biomaterials*, **25** (19), 4741–4748.

Woodfield, T.B.F., *et al.*, 2004. Design of porous scaffolds for cartilage tissue engineering using a three-dimensional fibre-deposition technique. *Biomaterials*, **25** (18), 4149–4161.